

NUMERICAL AND THEORETICAL INVESTIGATION ON COMPOSITE COLD-FORMED STEEL JOINTS WITH LIGHTWEIGHT CONCRETE

Cher Siang Tan*, Xiuwen Choo, Jian Jun Moy, Arizu Sulaiman

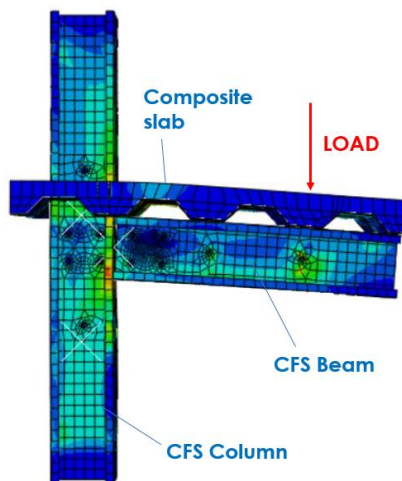
Faculty of Civil Engineering, Universiti Teknologi Malaysia, 81310
Johor Bahru, Johor, Malaysia

Article history

Received
29 March 2023
Received in revised form
18 May 2023
Accepted
19 May 2023
Published Online
21 August 2023

*Corresponding author
tcsiang@utm.my

Graphical abstract



Abstract

This research intends to investigate behaviour of composite cold-formed steel joint numerically through finite element analysis by using ABAQUS and theoretically by referring to BS 5950-1:2000 and Green book P213 "Joint in Steel Construction-Composite Connection". A composite joint is modelled by combination of composite beam and steel column with connection of HRS gusset plate and M12 bolts. The significant failure mode is local buckling in CFS column web which similar in experimental study, FEM numerical simulation and theoretical component calculation. The behaviour of the cold-formed steel composite joint will be expressed in moment-rotational and load-deflection relationship to determine the initial rotational stiffness and ultimate moment resistance. The findings from numerical and theoretical investigations are compared with the full-scale experimental study in three different thicknesses of gusset plate. A correlation in stiffness ratio and strength ratio are obtained in the range of 1.76 to 2.25, and 1.00 to 1.60 respectively indicating that the numerical modelling tends to underpredict the behaviour of the composite structures.

Keywords: Composite joint, finite element analysis, gusset plate, cold-formed steel, stiffness ratio

Abstrak

Penyelidikan ini bertujuan untuk mengaji tingkah laku sambungan komposit keluli bergulung sejuk (CFS) dengan menggunakan kaedah unsur terhingga (FEM) dengan menggunakan ABAQUS dan secara teori dengan merujuk kepada BS 5950-1:2000 dan Green Book P213 "Sambungan dalam Pembinaan Keluli - Sambungan Komposit". Sambungan komposit dimodelkan dengan gabungan komposit rasuk dan tiang keluli dengan sambungan plat gusset keluli tergelek panas (HRS) dan bolt M12. Mod kegagalan penting adalah kesan melengkung tempatan pada bahagian web tiang CFS yang serupa dalam kajian eksperimen, simulasi berangka FEM dan pengiraan komponen teoretikal. Tingkah laku sambungan komposit keluli bergulung sejuk akan dinyatakan dengan hubungan momen-rotasi dan beban-pesongan untuk menentukan kekakuan rotasi awal dan rintangan momen muktamad. Hasil daripada penyiasatan berangka dan teoretikal dibandingkan dengan kajian eksperimen skala asal dalam tiga ketebalan berbeza plat gusset. Perhubungan dalam nisbah kekakuan dan nisbah kekuatan diperolehi adalah dalam julat 1.76 hingga 2.25 dan 1.00 hingga 1.60 masing-masing, menyatakan bahawa simulasi berangka FEM cenderung untuk meramalkan tingkah laku sambungan komposit secara kurang tepat.

Kata kunci: Sambungan komposit, analisis elemen terhingga, plat gusset, keluli bergulung sejuk, nisbah kekakuan

© 2023 Penerbit UTM Press. All rights reserved

1.0 INTRODUCTION

Concrete and steel are the general structural materials that commonly used in construction sites. The usage of steel especially in cold-formed steel was widespread throughout the world. The design specifications were available and well established, for instance North American Specification for cold-formed steel design by American Iron and Steel Institute (AISI) [1] and Eurocode 3 Part 1-3 [2] that shows general rules in designing cold-formed thin gauge member and steel sheeting. Cold-formed steel is practical in secondary elements such as framing, rack, and truss industry. At the same time, it also continues to develop its function into new areas of mid-rise construction with additional shape and size options beyond its original cross-sections [3]. However, the members of CFS are vulnerable to buckling, torsional failure and compressions. The effectiveness of CFS can be improved significantly by combining with other types of building material to form composite structures [4]. In the system of composite structures, composite joints act as an important part in connection to enhance its structural stiffness and strength by providing a higher rotational stiffness and moment resistance.

Under steel and concrete composite structures, connection plays an important role to ensure the safety of the whole structure by enhancing the composite action between both steel and concrete components. A suitable connection can reduce the required member size and the material cost consequently. Composite joint able to resist the moment from gravitational load and act as hinges when there is existing of horizontal load. It is influenced by the structural interaction between reinforced concrete with steel sections that assess different global and local responses in actual geometrical and mechanical properties [5]. The different in behaviour of composite joints from bare joints is due to the composite action between reinforced concrete and steel joint can improve the moment resistance as well as rotational stiffness. The ultimate moment capacity and rotational stiffness of composite joint can be significantly influenced by various factors, such as the reinforcement ratio, type of steel and concrete, slenderness of the beam section, and the type of shear connector [6]. Furthermore, the study conducted by F. Amsyar *et al.* [7] found significant difference in the ultimate moment capacity, rotation, and initial stiffness when comparing non-composite and composite structures.

In the existing literature, several studies have investigated the structural behaviour of composite structures, which includes the moment capacity, rotational stiffness with varying parameters. Faridmehr *et al.* [8] conducted experimental tests on composite structures, varying parameters such as beam depths and types of connections. In contrast, Huei *et al.* [9] performed numerical studies using ABAQUS software to model composite structures and examined the

structural behaviour of the light gauge steel top-seat flange-cleat connection with different beam depths of 150 mm, 200 mm and 250 mm. However, limited data exists in the literature regarding the investigation of composite cold-formed steel (CFS) joints incorporating lightweight concrete. Additionally, the thickness of the gusset plate was varied in 2 mm, 4 mm and 8 mm to further explore its impact on the composite structures.

There will be a change in load distribution between the bolts when composite damage occurs [10]. The mechanical properties of composite joints require to withstand sufficient bearing strength and set dominant rupture mode with bearing failure mode. Net tension and shear out failure mode are the mode wherein capability of load transfer unable to remain in joint. The failure mode is classified based on ratio of different geometry of structure such as width, bolt hole diameter and edge distance [11]. The failure mode should be controlled and predict during the design of the joint structure to ensure the safety of structure and the improvement in weight-saving efficiency. The common failure reason is the loss of strength and stiffness in joints due to local buckling [12], concrete cracking [13], and beam torsional [14]. The failure mode in bolted joints can be categorized into progressive failure and immediate failure which can be represented by bearing failure and shear out failure respectively.

This study aims to investigate the behaviour of composite beam-to-column of CFS joint numerically through finite element analysis (FEA) software and theoretically based on component method. Furthermore, a composite joint with an optimum thickness of HRS gusset plate can be determined to enhance the strength and stiffness of connection within composite structural in maximum utilization of cold-formed steel and lightweight concrete by reducing the beam depth.

2.0 METHODOLOGY

2.1 Numerical Simulation

A refined FE numerical modelling was proposed by utilising ABAQUS 2017 [15] software to assess the structural responses of composite cold-formed steel joint. To produce a reliable numerical simulation, the computational composite joint model was compared with physical experimental results for validation purpose. Three finite element models were simulated based on different thicknesses of HRS gusset plate that were same as the experimental specimens tabulated in Table 1. The parameters other than HRS gusset plate thickness remained unchanged throughout the numerical simulation. STATIC, RISK step (arc-length method) and C3D8 (Continuum, 3-Dimensional, 8-node) [16] were selected to analyse and model the finite element model by referring to the study from previous

researchers [5, 7, 17-19]. The dimensions and material properties of the model are based on the data from the coupon tests based on ISO-6892 [20] to ensure consistency. The configuration of numerical simulation is same with the experimental data to simulate the actual behaviour of composite joint with different thicknesses of HRS gusset plate.

2.1.1 Modelling Specification (Dimension, Material Properties, and Mesh)

A total of 13 individual parts were modelled and assembled as a composite structure in ABAQUS. The dimensions and material properties of each part were modelled to be identical to the experiment specimen. Column and beam were created by the assembling of two back-to-back C-channels with bolts. The material properties of different parts such as elastic properties (Young's Modulus and Poisson's Ratio) and plastic properties (yield stress, ultimate stress, and plastic strain) were obtained from experimental coupon test. In addition, the parts were partitioned through datum plane to reduce the geometry complexity and perform a smoother mesh. Each partition of part can be assigned with different mesh size, boundary conditions, and interactions. Generally, global mesh size was assigned to every part. The modelling specification of all parts in term of dimension and mesh were shown in Table 2, whereby material properties tabulated in Table 3.

Table 1 Comparison Study of Experimental Specimen and Numerical Model

Models	Experiment Specimen Label	Thickness of HRS gusset plate (mm)
Model 1	S2-12-1200-100-T10	2
Model 2	S4-12-1200-100-T10	4
Model 3	S8-12-1200-100-T10	8

2.1.2 Contact Interaction and Constraints

Interaction is the relationship between different interface areas of model part that are in contact with each other. The model was simulated with surface-to-surface contact interaction that contacted between different areas on the same surface which made up of hard contact surface and tangential friction. The contact property option of normal behaviour with Hard Contact Pressure-Overclosure was selected for hard contact surface that applied between the connection and cross-sectional area of CFS beam and column flange surface, whereby friction interaction was created based on the contact surfaces induced friction coefficient of 0.3 and 0.5 for CFS steel and steel deck respectively. Besides, it was found that a special interaction of XFEM crack growth introduced a 500

mm width concrete crack in this model. The crack was allowed to be propagated in the simulation to investigate the actual behaviour of failure mode.

Table 2 Section Dimension and Mesh Size of Modelling Parts

Sections and Parts	Section Dimension (width x height)	Extrusion	Mesh Size
CFS Column	150 x 200	1200	34
CFS Beam	150 x 200	900	32
Profiled Deck	1200 x 1	500	28
LWC Slab	1200 x 100	500	36
HRS Gusset Plate	400 x 150	2, 4, 8	13
T10 Rebar (T) 210 mm	10 (diameter)	210	7
T10 Rebar (T) 450 mm	10 (diameter)	450	8
T10 Rebar (L) 850 mm	10 (diameter)	850	9
T10 Rebar (L) 1150 mm	10 (diameter)	1150	10
M12 Tension Bolt	12 (diameter)	4, 8, 12	3
Loading Plate	50 x 50	10	8
CFS Shear Connector	150 x 190	100	17
Concrete Crack (shell)	500	1	-

** All of the dimensions are in the unit of mm

Table 3 Material Properties of Modelling Part

Modelling Part	Elastic Properties		Plastic Properties	
	Young Modulus, (kN/mm ²)	Poisson's ratio, ν	Yield Stress, f_y (kN/mm ²)	Ultimate Stress, f_u (kN/mm ²)
Cold-formed Steel	198	0.3	0.555	0.60
Hot-rolled Steel	210	0.3	0.275	0.430
T10 Rebar LW	213.5	0.3	0.644	0.714
Concrete	25	0.2	-	-
M12 Bolt	210	0.3	0.800	0.911
Bare Steel Profile	210	0.3	0.275	0.430
Deck	210	0.3	0.664	0.690

** Lightweight concrete is input with the mass density of 1200 kg/m³, and 38.9 MPa for max principal stress which obtained from 28 days concrete compressive strength test.

Furthermore, the interaction constraints involved in this study were the tie, rigid body, and embedded region. A tie constraint allows two surface regions of different meshes to fuse together, which is the most common option for the bonding of different parts such as bolt shank, bolt surface and slab area in the model. Moreover, rigid body constraint limits the motion of the assembly region to the reference point which remains the same location throughout the analysis. "TIE (nodes)" was selected as the region type for all rigid body constraints especially at the location of loads applied to loading plate. Illustration of the modelling with details were shown in Figure 1. Besides, the embedded region constraint can embed a part of the model within the specific part, which is invisible from the overview of modelling. Both

rebars and upper part of shear connectors are embedded in the lightweight concrete slab.

2.1.3 Load and Boundary Condition

Based on laboratory setup, the end condition of the column was defined using the built-in ENCASTRE function in ABAQUS, where pinned for bottom and roller for top to resist the displacement and rotational at these two ending supports. A concentrated gravity point load of 1000 kN is applied at RP1 which directly acts on the loading plate with 700mm from the surface of column flange to induce moment. Besides, the loading plate and both sides of lightweight concrete slab are proposed to restrain the movement in Z-direction and ensuring the model to move in either x or y-directions. Furthermore, additional PINNED boundary condition was applied behind the slab to restrain the movement that that location. All the boundary conditions will be propagated from the initial step until the end of numerical simulation.

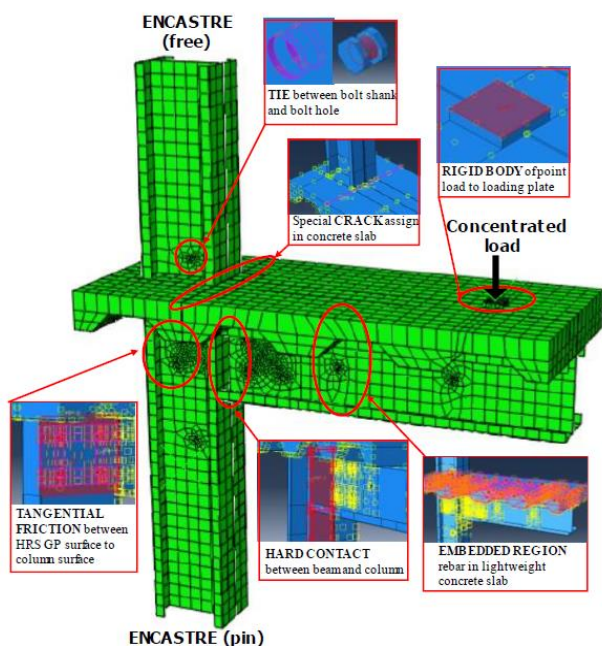


Figure 1 Example of interactions and constraints in FE modelling of composite joint

2.1.4 Structural Modelling and Analysis

Figure 2 shows the complete composite structure joint modelling with and without showing the lightweight concrete slab and CFS beam. The hidden part under the concrete slab includes the reinforcements, shear connectors and the gusset plate in between column and beam which were embedded in the slab region. The analysis results from the numerical simulation were tabulated in excel in term of Load, LVDT 1, LVDT 2, LVDT 3 and LVDT 4 for further analysis on the performance of the composite joint. The data were then converted into

load-deflection and moment-rotation relationships and plotted as L-d graphs and M- θ graphs, respectively. The behaviour of composite joints can be explained based on the moment rotational and load-deflection relationship to determine effect of HRS gusset plate thickness on the strength and stiffness of the composite joint.

2.2 Theoretical Study

Theoretical study was carried out to evaluate the composite action behaviour of the composite joint. Throughout the theoretical study, British Standard BS 5950-1:2000 [21] and Green book P213 "Joint in Steel Construction - Composite Connection" [22] were used as references in the moment capacity calculations. Component method was used to calculate moment capacity in each of the component individually in tension zone, compression zone and shear panel zone based on the relevant failure mode. The results from theoretical study were then compared and reviewed with experimental study to determine the structural behaviours in strength of composite joint with different thickness of HRS gusset plate.

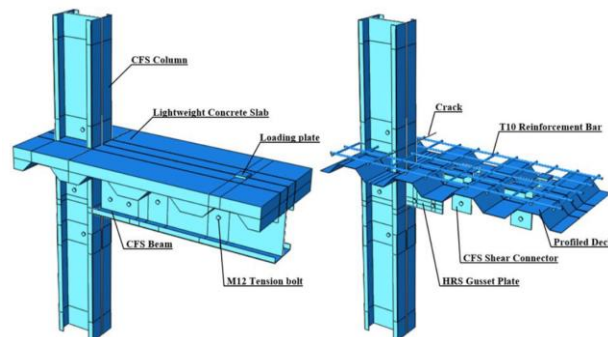


Figure 2 Finite Element Model of Composite Joint Created by ABAQUS

3.0 RESULTS AND DISCUSSION

3.1 Numerical Simulation

Numerical simulation of composite CFS joint with lightweight concrete is a highly iterative process to provide a quality prediction of composite joints' properties for different HRS gusset plate thickness others than conducting laboratory work. The numerical result by ABAQUS simulation were shown in failure mode and moment-rotational response to identify the initial rotational stiffness of composite joint.

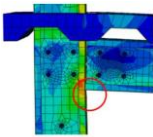
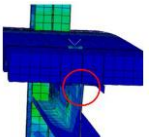
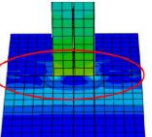

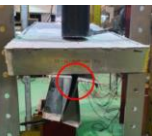

3.1.1 Failure Mode

The failure of composite joint generally were due to the poor resistance of concrete in tension and steel in compression when the load applied exceeded its capacity. Furthermore, cold-formed steel is a thin

layer of light-material which commonly fail under buckling failure mode. Von Mises stress was used to identify the critical location in the composite joint model. The greatest stress observed were 1687 MPa which occurred at the bolt in the middle of beam that connected with CFS shear connector. The deflection of the composite joint was due to the 100 kN loading applied at the loading plate, causing tension at the top surface and compression at the lower surface. Since the concrete is weak in tension, most of the tension was captured by the reinforcement in the slab. Although the concrete crack is created and allowed to growth during the modelling process, it is extended to other position but not only in vertical direction which led to additional failure of model.

Local buckling is the main failure occur which was found at the CFS column part that connecting with CFS beam lower web with the highest stress. The CFS sections buckle locally at the compression zone which reduced the strength and stiffness of overall composite structure and limits its load carrying capacity. The local buckling caused the CFS beam and CFS column to be shifted from their original configuration and formed a separation gap. Moreover, torsional buckling was observed at the free end of CFS beam when subjected to loading which divides the section into compression and tension region, creating different movement in the section. The tension part restrained the beam section to be straight while the compression region of the beam attempted to deflect it laterally and cause the beam to be twisted [23]. Since the CFS beam was modelled by two different C-lipped section with 2 mm flange and web thickness, the beam collided to each other at the lower part and separated away from each other at the top part when the torsional buckling effect is high. The comparison of failure mode between ABAQUS modelling and actual experiment specimens are illustrated in Table 4.

Table 4 Comparison of failure mode in numerical model and experimental specimen

Failure Mode	Local Buckling at the CFS column flange with lower beam web	Torsional Buckling of CFS beam end	Formation of Concrete Crack
Numerical Model			
Experimental Specimen			

3.1.2 Moment-rotational Response

Moment-rotational response able to present the behaviour of the composite joint in term of its initial rotational stiffness, moment capacity and rotational capacity. In this study, the initial rotational stiffness of the composite joint is focused to compare the results between numerical simulation and experimental result. In the experiment, moment rotational curve is obtained by collecting results from the inclinometers at the respective position on beam and column with the point load for record. Similarly, the data extracted from ABAQUS numerical simulation were based on the same LVDT 1, 2, 3, and 4 locations as the experimental. Moment in a structure represents the rotational effect of composite joint that obtained by the applied load multiple with its corresponding perpendicular distance, which is fixed as 700 mm from the column flange surface in this study. On the other hand, the rotation of composite joint was measured by the beam rotation subtracted to column rotation in radian unit. Based on the moment rotational graph, the initial stiffness can be represented by its gradient of the first slope of the induced moment against its corresponding rotational. Figure 3 displayed the moment-rotational graph of three different thicknesses of gusset plate experimentally and numerically.

3.2 Comparison of Initial Rotational Stiffness of Composite Joint between Experimental and Numerical Results

The initial rotational stiffnesses were tabulated in Table 5 to show the comparison between the experimental and numerical as well as their stiffness ratio. It is represented by the elastic range of the moment-rotational curve that shows the rigidity of the composite joint. Overall, experimental results yields a greater initial rotational stiffness than numerical simulation in three of the HRS gusset plate thicknesses. Table 5 shows that the initial rotational stiffness is increasing proportionally when the HRS gusset plate become thicker in both experimental and numerical results by providing higher rigidity to the composite joints. The experimental results shows a nearly straight slope based on the plots in Figure 3 and followed by non-linear incremental in rotational due to the formation of concrete cracks on the specimens. The response from experimental specimen almost reaches horizontal after ultimate moment in both 2 mm and 4 mm HRS gusset plate thicknesses specimens that indicating the composite joint slipping because of the excessive deformation. Apart from experimental results, numerical results exhibited a smooth curve with linear slope at the beginning and gradually losing its stiffness as the rotation of the structure increased. The loss in rotational stiffness occurred when there is failure in the composite joint components such as shear off failure.

Table 5 Initial Rotational Stiffness of different thickness of HRS Gusset Plate

HRS Plate thickness	Gusset	Initial Rotational Stiffness (kNm/rad)		Stiffness Ratio
		Experimental	Numerical	
2 mm		774.0	440.75	1.76
4 mm		1296.06	576.62	2.25
8 mm		1300.31	656.28	1.98

3.3 Theoretical Study in the Moment Capacity of Composite Joint

Moment capacity represents the strength of composite joint that is important in obtaining the ultimate resistance that composite joint able to resist before corruption of composite structure occur. Moment capacity of theoretical study was carried out by component approach referred to BS 5950-1:2000 [21] and Green book P213 [22]. Component method is defined as the moment capacity of each component which are calculated individually in tension zone, compression zone and shear panel zone based on the relevant failure mode. The lowest value among these three zones will be indicated as the moment capacity of the composite joint because it indicated the first failure that will occur in the composite joint. Tension zone will be contributed by reinforcement and HRS gusset plate, where compression zone will be chosen among the lowest value among column web crushing, column web buckling and beam flange crushing failure. Besides, shear panel zone is required to include due to the composite joint in this study is one-sided, which will cause resultant panel to shear due to its asymmetry.

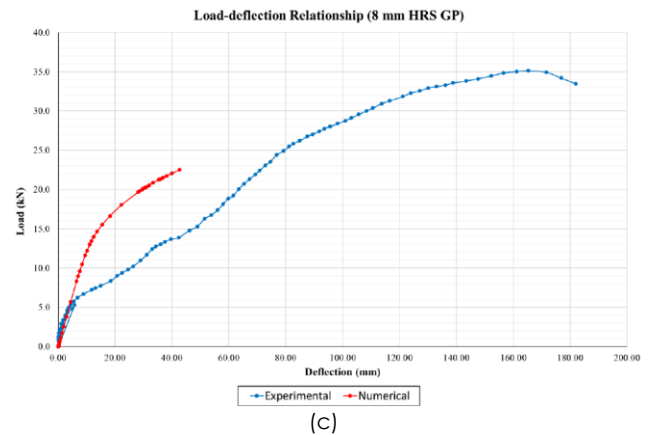
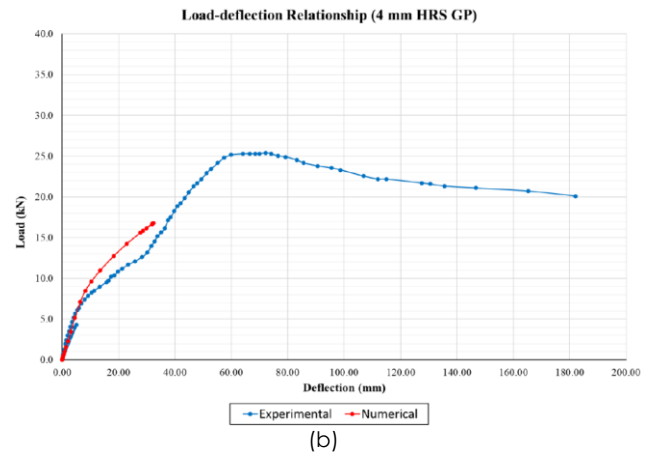
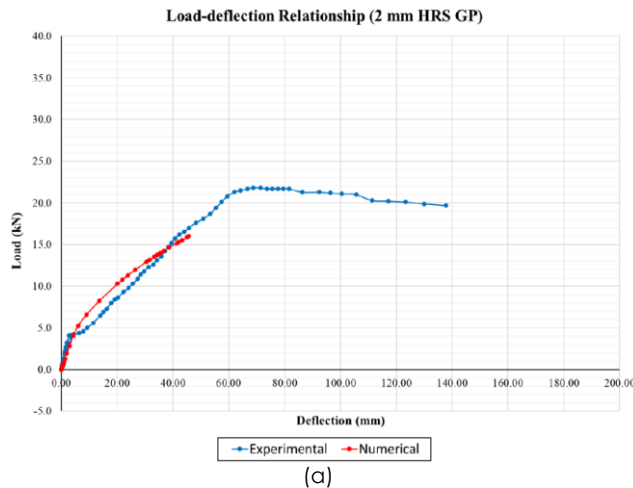


Figure 3 Moment-Rotational relationship between experimental and numerical results in HRS GP thickness of (a) 2 mm, (b) 4 mm, (c) 8 mm

3.4 Comparison of Moment Capacity of Composite Joint between Experimental and Theoretical Results

Based on theoretical results, the moment capacity is only changed in tension zone along with different HRS gusset plate thickness. The moment capacity in compression zone and shear zone are remained as 15.35 kNm and 53.280 kNm respectively. This was due to the tension zone governed by reinforcement in the concrete slab and HRS gusset plate in between the column and beam C lipped section. Hence, the changes in the parameter of gusset plate only affect the moment capacity in tension zone. However, only a small increment of moment capacity in tension zone as the HRS gusset plate thickness is increasing from 2 mm to 8 mm. By referring to the theoretical calculation, reinforcement contributed the majority moment capacity in tension zone.

Table 6 Moment Capacity of different thickness of HRS Gussety Plate

HRS Gusset Plate thickness	Moment Capacity (kNm)		Strength Ratio
	Experimental	Numerical	
2 mm	15.28	15.35	1.00
4 mm	17.78	15.35	1.16
8 mm	24.59	15.35	1.60

The most critical zone to initiate the failure mode in composite joint was controlled by the compression zone, which able to provide moment capacity of 15.35 kNm in column web buckling failure mode. Since the ultimate moment capacity was affected by compression zone, the change in HRS gusset plate thickness will not influence to the ultimate moment capacity of the composite joint. As the thickness of HRS gusset plate increases, the moment capacity of entire composite joint remained as 15.35 kNm theoretically, however it is increasing experimentally. Hence, the strength ratio between theoretical and experimental results were increased as shown in Table 6.

4.0 CONCLUSION

This research study aims to enhance the knowledge in both development and analysis of composite joint. The performance of a composite structure was highly depended on its composite joint to form a stable and safe structure. The main failure mode of composite joint was shown as the local buckling at the column web which was proved in experimental, numerical and theoretical results. Furthermore, the thickness of the 8 mm gusset plate performed the greatest structural behaviour in steel-concrete composite joint compared to the other thicknesses of the gusset plate due to higher initial stiffness in thicker gusset plate referring to numerical analysis. However, theoretical analysis that used to investigate the moment capacity of composite joint shown that the thickness in gusset plate was not a significant factor. Tension zone provides the higher strength to composite joint that able to uphold greater moment capacity than compression zone. Since the theoretical analysis is using component approach, the moment capacity of composite joint was governed by compression zone, which contributed by CFS column and beam. In overall, it can be concluded that the results obtained from both numerical and theoretical evaluation were lower than of the experimental results with stiffness ratio ranging from 1.76 to 2.25 and strength ratio of 1.00 to 1.60 respectively. With the ratios having values higher than 1.00, it indicates that the numerical modelling underestimated the structural behaviour of the composite structure. Therefore, in further study, it is recommended to propose a modification factor and

safety factor to improve the conservatism in the analysis and design.

Conflicts of Interest

The author(s) declare(s) that there is no conflict of interest regarding the publication of this paper.

Acknowledgement

The authors would like to express appreciation for the financial support of Universiti Teknologi Malaysia (UTM-FR 21H47 and 21H68).

References

- [1] G. J. Hancock, T. Murray, and D. S. Ellifrit. 2001. *Cold-formed Steel Structures to the AISI Specification*. CRC Press. Doi: <https://doi.org/10.1201/9780203907986>.
- [2] BSI. 2005. 1993-1-1: 2005 Eurocode 3: Design of Steel Structures – Part 1-1: General Rules and Rules for Buildings. *European Committee for Standardisation*.
- [3] B. Schafer. 2011. Cold-formed Steel Structures around the World. *Steel Construction*. 4: 141-149. Doi: <https://doi.org/10.1002/stco.201110019>.
- [4] G. J. Hancock. 2003. Cold-formed Steel Structures. *Journal of Constructional Steel Research*. 59(4): 473-487. Doi: [https://doi.org/10.1016/S0143-974X\(02\)00103-7](https://doi.org/10.1016/S0143-974X(02)00103-7).
- [5] C. Amadio, C. Bedon, M. Fasan, and M. Pecce. 2017. Refined Numerical Modelling for the Structural Assessment of Steel-concrete Composite Beam-to-column Joints under Seismic Loads. *Engineering Structures*. 138: 394-409. Doi: <https://doi.org/10.1016/j.engstruct.2017.02.037>.
- [6] Y. Song, J. Wang, B. Uy, and D. Li. 2021. Behaviour and Design of Stainless Steel-concrete Composite Beam-to-Column Joints. *Journal of Constructional Steel Research*. 184: 106800. Doi: <https://doi.org/10.1016/j.jcsr.2021.106800>.
- [7] F. Amsyar, T. C. Siang, A. Sulaiman, and M. C. Khun. 2020. Numerical and Experimental Study of Semi-rigid Beam-to-column Composite Connections in Cold-formed Steel. *AIP Conference Proceedings*. 2284(1): 020011.
- [8] I. Faridmehr, M. M. Tahir, M. H. Osman, A. F. Nejad, and R. Hodjati. 2015. An Experimental Investigation of Stiffened Cold-formed c-channels in Pure Bending and Primarily Shear Conditions. *Thin-Walled Structures*. 96(4): 39-48. Doi: <https://doi.org/10.1016/j.tws.2015.07.023>.
- [9] L. Y. Huei, T. C. Siang, M. M. Tahir and S. Mohammad. 2012. Numerical Modelling and Validation of Light Gauge Steel Top-seat Flange-clip Connection. *Journal of Vibroengineering*. 14(3): 1104-1112. <https://www.extrica.com/article/10666>.
- [10] X. Cheng, S. Wang, J. Zhang, W. Huang, Y. Cheng, and J.-k. Zhang. 2017. Effect of Damage on Failure Mode of Multi-bolt Composite Joints using Failure Envelope Method. *Composite Structures*. 160: 8-15. Doi: <https://doi.org/10.1016/j.compstruct.2016.10.042>.
- [11] D. Yoon, S. Kim, J. Kim, and Y. Doh. 2020. Study on Bearing Strength and Failure Mode of a Carbon-epoxy Composite Laminate for Designing Bolted Joint Structures. *Composite Structures*. 239:112023. Doi: <https://doi.org/10.1016/j.compstruct.2020.112023>.
- [12] B. Uy and M. A. Bradford. 1995. Local Buckling of Cold Formed Steel in Composite Structural Elements at Elevated Temperatures. *Journal of Constructional Steel Research*. 34(1): 53-73. Doi: [https://doi.org/10.1016/0143-974X\(94\)00021-9](https://doi.org/10.1016/0143-974X(94)00021-9).

- [13] J. M. Irwan, A. H. Hanizah, I. Azmi, and H. B. Koh. 2011. Large-scale Test of Symmetric Cold-formed Steel (CFS)-Concrete Composite Beams with BTST Enhancement. *Journal of Constructional Steel Research*. 67(4): 720-726. Doi: <https://doi.org/10.1016/j.jcsr.2010.11.008>.
- [14] K. M. Aminuddin, A. Saggaff, and M. M. Tahir. 2017. Experimental Behaviour of Beam-column Connection using Cold-formed Steel Sections with Rectangular Gusset-plate. *AIP Conference Proceedings*. 1903(1): 020006. Doi: <https://doi.org/10.1063/1.5011486>.
- [15] D. Systemes. 2017. Abaqus CAE - Finite Element Modeling, visualization, and process automation. URL: <https://www.3ds.com/products-services/simulia/products/abaqus/abaquscae/>.
- [16] M. Smith. 2009. ABAQUS/Standard User's Manual, Version 6.9.
- [17] F. Amsyar, C. S. Tan, S. Mohammad, M. M. Tahir, and H. A. Hamid. 2021. Partial Strength Beam-to-column Connection of Cold-formed Single Channel Section: Numerical and Experimental Study. *ASM Science Journal*. 14: 1-11. Doi: <https://doi.org/10.32802/asmscj.2020.639>
- [18] A. Ataei and M. A. Bradford. 2014. Finite Element Analysis of Sustainable and Deconstructable Semi-rigid Beam-to-Column Composite Joints. *The 5th International Conference on Computational Methods*. 1-10
- [19] C. Amadio, C. Bedon, and M. Fasan. 2017. Numerical Assessment of Slab-interaction Effects on the Behaviour of Steel-concrete composite joints. *Journal of Constructional Steel Research*. 139: 397-410. Doi: <https://doi.org/10.1016/j.jcsr.2017.10.003>.
- [20] ISO, E. 2001). 6892-1: 2016 Metallic materials-Tensile testing-Part 1: Method of test at room temperature (ISO 6892-1: 2016). European Committee for Standardization.
- [21] BSI. 2001. 5950-1: 2000. Structural Use of Steelwork in Building – Part 1: Code of Practice for Design – Rolled and Welded Sections. Standards Committee.
- [22] G. H. Couchman and A. G. Way. 1998. SCI P213 – Joints in Steel Construction: Composite Connections. Steel Construction Institute.
- [23] A. Paul. 2014. Lateral Torsional Buckling in Beams: Lateral Deflection and Torsion. <https://civildigital.com/lateral-torsional-buckling-beams-lateral-deflection-torsion/>.